# Stress Wave Propagation in 2D Functionally Graded Media: Optimization of Materials Distribution

**Parham Rajabi**[1]
Department of Mechanical Engineering,
University of Sistan and Baluchestan, Zahedan, Iran
E-mail: n.rajaby45@gmail.com

**Hossein Rahmani**[2, *]
Department of Mechanical Engineering,
University of Sistan and Baluchestan, Zahedan, Iran
E-mail: H_Rahmani@eng.usb.ac.ir
*Corresponding author

**Alireza Amiri**[3]
Department of Mechanical Engineering,
University of Sistan and Baluchestan, Zahedan, Iran
E-mail: Alireza_Amiri@pgs.usb.ac.ir

**Received: 5 September 2020, Revised: 17 November 2020, Accepted: 1 December 2020**

**Abstract:** In this paper, the analysis and optimization of the effect of the materials distribution on the behavior of 2D functionally graded media subjected to impacted loading has been investigated. First, it is assumed that there are two cases for distributing the components in the FG material. In the first case, the power law is considered for materials distribution, and in the second case, the volume fractional changes of the components are made by third degree interpolation. Considering the elastodynamic behavior of the FG materials under loading, the general governing equations of the wave propagation are extracted for the case of properties variation in two dimensions and then the equations are solved using the finite difference method. Finally, an optimization has been made using a single objective genetic algorithm. The results show that the materials distribution has a considerable effect of stress wave propagation in FGMs.

**Keywords:** Functionally Graded Material, Finite Difference Method, Genetic Algorithm, Optimization, Stress Wave Propagation

**Reference:** Parham Rajabi, Hossein Rahmani, and Alireza Amiri, "Stress Wave Propagation in 2D Functionally Graded Media: Optimization of Materials Distribution ", Int J of Advanced Design and Manufacturing Technology, Vol. 14/No. 2, 2021, pp. 49-63. DOI: 10.30495/admt.2021.1908681.1216

**Biographical notes: Parham Rajabi** is a M.Sc. candidate of Mechanical Engineering at the University of Sistan and Baluchestan, Zahedan, Iran. His current research interest includes impact engineering and optimization. **Hossein Rahmani** received his Ph.D. in Mechanical Engineering from Semnan University in 2014. He is currently Assistant Professor at the Department of Mechanical Engineering, University of Sistan and Baluchestan, Zahedan, Iran. His current research interest includes impact engineering and elastodynamic. **Alireza Amiri** is M.Sc. graduated in Mechanical Engineering from University of Sistan and Baluchestan, Zahedan, Iran. His finial M.sc. thesis was about stress wave propagation in FGMs.

 

## 1 INTRODUCTION

Layer composites, despite their favorable thermal and mechanical properties, have some disadvantages at high temperatures such as failure due to shrinkage and stress concentration due to rapid changes in material properties at the interface between them. FG materials, in which mechanical and thermal properties are constantly changing gradually, are suitable options for solving this problem. In recent years, FG materials have been widely used in aerospace industries, high-temperature environments such as nuclear reactors and chemical equipment [1]. Principally in most engineering applications, FG materials are formed from two phase metal and ceramic, but the amount and type of placement of FG material components to reduce stress concentration and improve material resistance are very important issues that have been neglected [2-6].

To date many scholars have investigated FG materials. Goupee et. al [7] provided two-dimensional optimization for the production of FGM materials using a non-network method and a genetic algorithm. Due to the fact that this type of material exhibits good performance in difficulty conditions, the proposed method focuses on metal-ceramic materials. Zhang et al. [8] investigated the wave propagation and the dynamic response of a layered inhomogeneity structure using finite element method. They examined the general changes in the properties of material such as density, Poisson's coefficient, and elastic modulus at each element's surface using a general parametric formulation.

Hosseini et al. [9], presented numerical simulation of the emitting wave propagation in heterogeneous continuous material. In their research, the propagation of stress and displacement wave was investigated in a one-dimensional FGM material that was affected by a load. The governing equations were obtained on the FGM plate which was hit by the loading, and the numerical method, which was based on the differential method, was used to simulate the stress and displacement wave in a one-dimensional FGM plate with different boundary conditions. Cao et al. [10] studied the propagation of the lamb wave in functionally graded media using the power series technique. In order to investigate the behavior of the lamb waves propagating in the FG media which was affected by thermal stress and its mechanical properties continuously were changed along the thickness, the power series method, whose high convergence and high accuracy were proven, was used to derive theoretical results. Sun et al. [11] examined wave propagation and transient response of the FG plate under the impact in the thermal environment. It should be noted that the FG plate was considered infinitely, and also the effects of temperature were discussed. Using the results of this study, they found that the frequency and velocity of wave propagation on FG plates were significantly reduced by increasing the surface temperature of the plate. Noh et al. [12] examined a reliable design that was based on the optimization of the distribution of volume fractions in functionally graded materials. In this optimization method, a limited number of volume fractions of different layers of the FG material and its material properties as a variable were considered. Using the results of the numerical experiments that the desired optimization method was used in them, they presented an optimal volume fraction distribution that was highly reliable and applicable at the stages of targeted material production. Zafarmand and his colleague [13] presented a three-dimensional dynamic and propagation of the stress wave on thick plates against impact load. In their research, the mechanical properties of the material (elasticity and density modulus) are continuously in line with thickness and based on the power distribution and the Poisson ratio is assumed to be constant. Also, Asgari [14], optimized material in a heterogeneous cylinder intended for wave propagation. He optimized the distribution of volume fractions in a hollow thick heterogeneous cylinder which was subjected to internal compression loading. The volume fractions of the materials in the limited number of design points were considered as variables and at each optional point in the cylinder were obtained by means of third degree interpolation functions. Two functions were considered for optimization. 1- Optimization of stress wave size in the material at specified time interval. 2- Optimization of displacement at the outer surface of the cylinder. To find the general solution of the problem, optimizing a multi-objective genetic algorithm with an internal finite element function was used. Daneshjou et al. [3] examined wave propagation and transient response of a functionally graded cylinder filled with liquid and rigid core using the inverse Laplace transform method. The equations of motion were extracted according to the definition of the problem as a plain strain. Using numerical results, they found that with the increase in the radius of the rigid core, von Mises stress was significantly reduced. Bednarik et al. [15] examined propagation of the one-dimensional longitudinal elastic waves in line with the thickness of a plate made of FG materials. Amiri et.al [16] investigated the effect of material distribution on torsional stress wave propagation. Yang and Liu [17] proposed a new boundary element method for modeling 2-D wave propagation problems in FGM materials in frequency domain. They investigated gradation direction and frequency on the wave propagation.

In this research, the finite difference method is used to study the propagation of two-dimensional wave in a functionally graded material. To distribute the

constructive elements of the material, two distribution modes are used: 1- The power law distribution and 2- Third degree interpolation. In the following, using a single-objective genetic algorithm, optimizing the volume fractions of the material and the type of distribution are discussed. Then, the components of displacement, strain, and stress diagrams have been discussed. The main novelty of this research is finding and optimizing the material distribution in FGMs so that when stress wave propagates on it, the stress in different point reduces to the least possible amount.

## 2 MODELING PROCEDURE

In this section, the equations for the 2D wave propagation in functionally graded plate will be extracted. In this paper, two different modes have been considered for obtaining volume fractions.

**First case:**

The FG plate discussed in this study consists of several gradient phases. This means that the FG plate consists of four different materials, as shown in "Fig. 1" , two materials used in this plate are ceramics ($c_1$, $c_2$ ) and two other materials are metals ($m_1$, $m_2$).

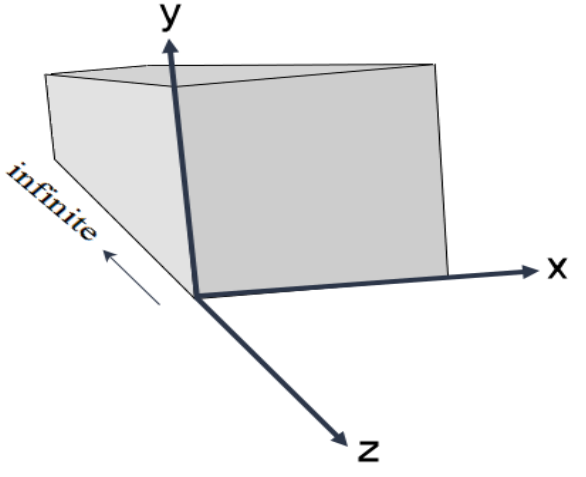


**Fig. 1** Cartesian coordinate with 2D material distribution.

The volume fraction of each one of the elements used in this FG plate can be obtained by "Eq. (1)" [18]:

$$V_{m1}(x,y)=[1-(\frac{x}{L_x})^{n_x}][1-(\frac{y}{L_y})^{n_y}]$$
$$V_{c1}(x,y)=[1-(\frac{x}{L_x})^{n_x}][(\frac{y}{L_y})^{n_y}] \quad (1)$$
$$V_{m2}(x,y)=[(\frac{x}{L_x})^{n_x}][(\frac{y}{L_y})^{n_y}]$$
$$V_{c2}(x,y)=[(\frac{x}{L_x})^{n_x}][1-(\frac{y}{L_y})^{n_y}]$$

To use volume fractions, the following rules in "Eq. (2)" should be considered [14]:

$$\begin{aligned} &Vc_1+Vc_2+Vm_1+Vm_2=1\\ &0\le Vc_1\le 1\\ &0\le Vc_2\le 1\\ &0\le Vm_1\le 1\\ &0\le Vm_2\le 1 \end{aligned} \quad (2)$$

**Second case:**

In the previous case, the volume fractions are defined by the power law function, and since the linear distribution of the volume fractions of the four materials is not necessarily the optimal distribution of the volume fractions, in the second case, the distribution of materials will be optimized so that the mechanical properties of the material will be improved. The volume fraction of each material in the second case in the Cartesian coordinates $D=[x_1x_2...x_m]\times[y_1y_2...y_n]$ is obtained from the equation 3 [19]:

$$\begin{aligned} V(x,y)=\sum_{p=0}^{1}\sum_{q=0}^{1}[&V^{(i+p,j+q)}H_{1+p}^{i}(x)H_{1+q}^{j}(y)\\ &+V_{,x}^{(i+p,j+q)}H_{3+p}^{i}(x)H_{1+q}^{j}(y)\\ &+V_{,y}^{(i+p,j+q)}H_{1+p}^{i}(x)H_{3+q}^{j}(y)\\ &+V_{,xy}^{(i+p,j+q)}H_{3+p}^{i}(x)H_{3+q}^{j}(y)] \end{aligned} \quad (3)$$

In this regard, the H functions are basically Hermitian functions, $V_{,x}$ indicates the derivation of $V$ with respect to $x$ and $V_{,y}$ is the derivation of $V$ with respect to y and $V_{,xy}$ shows the derivation with respect to $x$ and $y$.

### 2.1. Governing Equation

A FG plate, as shown in "Fig. 2" with specific length and width $L$, is considered and the properties of the constituent materials in the longitudinal and transverse directions are varying. The problem is expressed in Cartesian coordinates (x, y, z).

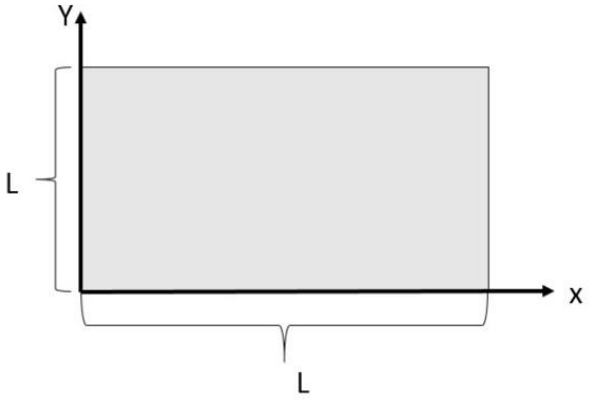


**Fig. 2** Functionally graded plate in Cartesian coordinates.

The 3D governing equations of motion in Cartesian coordinates for this FG plate is given in "Eq. (4)" [20]:

$$\begin{aligned}
&\frac{\partial T_{xx}}{\partial x}+\frac{\partial T_{xz}}{\partial z}+\frac{\partial T_{xy}}{\partial y}=\rho\frac{\partial^2 u}{\partial t^2}\\
&\frac{\partial T_{yy}}{\partial y}+\frac{\partial T_{yz}}{\partial z}+\frac{\partial T_{xy}}{\partial x}=\rho\frac{\partial^2 v}{\partial t^2}\\
&\frac{\partial T_{zz}}{\partial z}+\frac{\partial T_{yz}}{\partial y}+\frac{\partial T_{xz}}{\partial x}=\rho\frac{\partial^2 w}{\partial t^2}
\end{aligned} \tag{4}$$

Where, *u*, *v* and *w* are the displacement components, the stress components are defined by displacements as follows [21]:

$$\begin{aligned}
T_{xx}&=\lambda\left(\frac{\partial u}{\partial x}+\frac{\partial v}{\partial y}+\frac{\partial w}{\partial z}\right)+2\mu\left(\frac{\partial u}{\partial x}\right)\\
T_{yy}&=\lambda\left(\frac{\partial u}{\partial x}+\frac{\partial v}{\partial y}+\frac{\partial w}{\partial z}\right)+2\mu\left(\frac{\partial v}{\partial y}\right)\\
T_{zz}&=\lambda\left(\frac{\partial u}{\partial x}+\frac{\partial v}{\partial y}+\frac{\partial w}{\partial z}\right)+2\mu\left(\frac{\partial w}{\partial z}\right)\\
T_{xy}&=\mu\left(\frac{\partial u}{\partial y}+\frac{\partial v}{\partial x}\right)\\
T_{xz}&=\mu\left(\frac{\partial w}{\partial x}+\frac{\partial u}{\partial z}\right)\\
T_{yz}&=\mu\left(\frac{\partial w}{\partial y}+\frac{\partial v}{\partial z}\right)
\end{aligned} \tag{5}$$

Where, $T_{xx}$, $T_{yy}$ and $T_{zz}$ are normal stresses in x, y and z directions respectively, $T_{xy}$, $T_{yz}$ and $T_{xz}$ are shear stress components. $\lambda$ and $\mu$ are lame constants that are expressed in terms of:

$$\begin{aligned}
\lambda(x,y)&=\frac{E(x,y)\nu(x,y)}{(1-2\nu(x,y))(1+\nu(x,y))}\\
\mu(x,y)&=\frac{E(x,y)}{2(1+\nu(x,y))}
\end{aligned} \tag{6}$$

For a two-dimensional wave, displacement vectors are defined as follows:

$$\begin{aligned}
u&=u(x,y,t)\\
v&=v(x,y,t)\\
w&=0
\end{aligned} \tag{7}$$

When the "Eq. (5)" is replaced in "Eq. (4)", the equations are as follows:

$$\begin{aligned}
&\left(\lambda+2\mu\right)\frac{\partial^2 u}{\partial x^2}+\mu\frac{\partial^2 u}{\partial y^2}+(\lambda+\mu)\frac{\partial^2 v}{\partial x\partial y}+\\
&\left(\lambda_x+2\mu_x\right)\frac{\partial u}{\partial x}+\mu_y\left(\frac{\partial u}{\partial y}+\frac{\partial v}{\partial x}\right)+\lambda_x\frac{\partial v}{\partial y}=\rho\frac{\partial^2 u}{\partial t^2}\\
&\left(\lambda+2\mu\right)\frac{\partial^2 v}{\partial y^2}+\mu\frac{\partial^2 v}{\partial x^2}+(\lambda+\mu)\frac{\partial^2 u}{\partial x\partial y}+\\
&\left(\lambda_y+2\mu_y\right)\frac{\partial v}{\partial y}+\mu_x\left(\frac{\partial v}{\partial x}+\frac{\partial u}{\partial y}\right)+\lambda_y\frac{\partial u}{\partial x}=\rho\frac{\partial^2 u}{\partial t^2}
\end{aligned} \tag{8}$$

**2.2. Boundary Condition and Initial Condition**

Initial conditions are indicated at $t = 0$ as "Eq. (9)":

$$\begin{aligned}
u(x,y,t)&=0\\
v(x,y,t)&=0
\end{aligned} \tag{9}$$

Governing boundary condition in "Eq. (9)" at ( $0\le x\le a$ ) and ( $0\le y\le b$ ):

$$u(x,y,t)=\frac{F(t)\Delta t}{\rho c_l} \qquad \text{In } (x=0) \tag{10}$$

In "Eq. (10)", $\rho$ is the density and $c_l$ is the longitudinal wave speed. The following boundary conditions are also considered:

$$\begin{aligned}
&\frac{\partial u}{\partial y}(x,y,t)=0 && \text{In } (y=0)\\
&u(x,y,t)=0 && \text{In } (x=a)\\
&\frac{\partial u}{\partial y}(x,y,t)=0 && \text{In } (y=b)
\end{aligned} \tag{11}$$

**2.3. Loading Condition**

It is assumed that the plate is subjected to a time pulse loading. The variation of this load is defined in terms of time as "Eq. (12)".

$$P(t)=\begin{cases}\dfrac{1\times10^{6}}{10\times10^{-6}}t & t\le10\times10^{-6}(s)\\ \dfrac{-1\times10^{6}}{10\times10^{-6}}(t-20\times10^{-6}) & \\ & 10\times10^{-6}(s)<t\le20\times10^{-6}(s)\\ 0 & t>20\times10^{-6}(s)\end{cases} \quad (12)$$

Figure 3 presents the graph of this loading in terms of time.

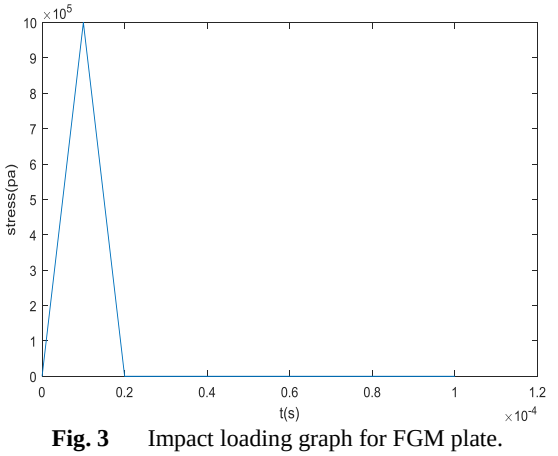


**Fig. 3** Impact loading graph for FGM plate.

## 3 FINITE DIFFERENCE METHOD

Different analytical and numerical methods can be used to solve wave equations. One of the numerical methods used to solve a wave equation is the finite difference method. This method is based on the Taylor expansion and the simple application of derivative definition. In short, the explanation of this approach shows that the space is fully divided to equal distances. Afterwards, all space is created by points. Then, by introducing the initial conditions and boundary conditions, the properties of all points will be obtained. In this research, the explicit central difference method is used [22].

### 3.1. Approximation of the Central Difference Method

First, we make the following important statement about the derivatives of partial differential equations:

Derivatives in the partial differential equation are approximated using the linear combination of function values in the network points.


**Fig. 4** A domain grid for specific interval 0 to X.

Using derivative fundamental definition and according to "Fig. 4", the first derivative of the first order for the hypothesized function is computed as follows:

$$\begin{aligned}\frac{\partial u}{\partial x}(\bar{x}) &= \lim_{\Delta x\to0}\frac{u(\bar{x}+\Delta x)-u(\bar{x})}{\Delta x}\\ &= \lim_{\Delta x\to0}\frac{u(\bar{x})-u(\bar{x}-\Delta x)}{\Delta x}\\ &= \lim_{\Delta x\to0}\frac{u(\bar{x}+\Delta x)-u(\bar{x}-\Delta x)}{2\Delta x}\end{aligned} \quad (13)$$

Using the definition of "Eq. (13)" for the second-order derivative, we have:

$$\begin{aligned}\frac{\partial^2 u}{\partial x^2} &= \left[\frac{\partial}{\partial x}\left(\frac{\partial u}{\partial x}\right)\right]=\\ &= \lim_{\Delta x\to0}\frac{\dfrac{u_{i+1}-u_i}{\Delta x}-\dfrac{u_i-u_{i-1}}{\Delta x}}{\Delta x}\\ &= \lim_{\Delta x\to0}\frac{u_{i+1}-2u_i+u_{i-1}}{(\Delta x)^2}\end{aligned} \quad (14)$$

According to "Fig. 5", the derivation with respect to x and y is calculated from the following relation:

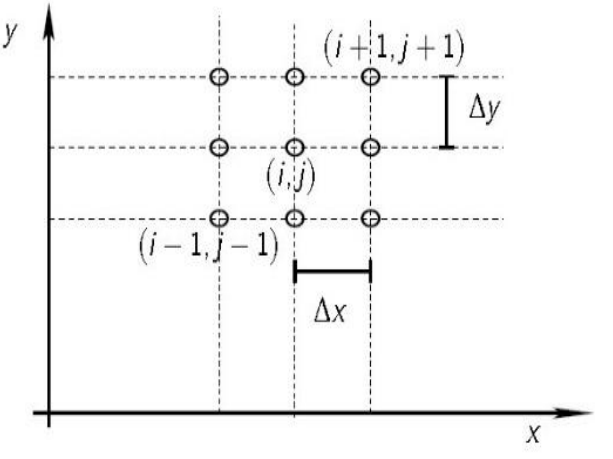


**Fig. 5** Two-dimensional networking in Finite difference method [22].

$$\frac{\partial^2 u}{\partial x\,\partial y}=\frac{u_{i+1,j+1}-u_{i-1,j+1}+u_{i-1,j-1}-u_{i+1,j-1}}{4\Delta x\,\Delta y} \quad (15)$$

Since in the finite difference method, the time interval is also regular networking, the time derivative of the desired function can be calculated in the same way.
The centered-difference equations of the second-order derivatives of a displacement component, such as $u(x, y, t)$ and $v(x, y, t)$ at the node $(i, j)$ with respect to time $t$ are given by:

$$\frac{\partial^2 u}{\partial t^2}=\frac{u_{i,j}^{k+1}-2u_{i,j}^{k}+u_{i,j}^{k-1}}{(\Delta t)^2}$$
$$\frac{\partial^2 v}{\partial t^2}=\frac{v_{i,j}^{k+1}-2v_{i,j}^{k}+v_{i,j}^{k-1}}{(\Delta t)^2} \quad (16)$$

$\Delta t$ is the size of the time interval, $k$ refers to the time index and $i, j$ indicate the position of the points in the network.
That way, the finite difference equations of the second-order derivatives of the displacement components $u(x, y, t)$ and $v(x, y, t)$ at the node $(i, j)$ with respect to the spatial variables $x$ and $y$ are shown in "Eq. (17)" [23]:

$$\frac{\partial^2 u}{\partial x^2}=\frac{u_{i+1,j}^{k}-2u_{i,j}^{k}+u_{i-1,j}^{k}}{(\Delta x)^2}$$
$$\frac{\partial^2 v}{\partial x^2}=\frac{v_{i+1,j}^{k}-2v_{i,j}^{k}+v_{i-1,j}^{k}}{(\Delta x)^2}$$
$$\frac{\partial^2 u}{\partial y^2}=\frac{u_{i,j+1}^{k}-2u_{i,j}^{k}+u_{i,j-1}^{k}}{(\Delta y)^2} \quad (17\text{-a})$$
$$\frac{\partial^2 v}{\partial y^2}=\frac{v_{i,j+1}^{k}-2v_{i,j}^{k}+v_{i,j-1}^{k}}{(\Delta y)^2}$$

$$\frac{\partial u}{\partial x}=\frac{u_{i+1}-u_{i-1}}{2\Delta x}\ ,\ \frac{\partial v}{\partial x}=\frac{v_{i+1}-v_{i-1}}{2\Delta x}$$
$$\frac{\partial u}{\partial y}=\frac{u_{j+1}-u_{j-1}}{2\Delta y}\ ,\ \frac{\partial v}{\partial y}=\frac{v_{j+1}-v_{j-1}}{2\Delta y} \quad (17\text{-b})$$
$$\frac{\partial \lambda}{\partial x}=\frac{\lambda_{i+1}-\lambda_{i-1}}{2\Delta x}\ ,\ \frac{\partial \mu}{\partial x}=\frac{\mu_{i+1}-\mu_{i-1}}{2\Delta x}$$
$$\frac{\partial \lambda}{\partial y}=\frac{\lambda_{j+1}-\lambda_{j-1}}{2\Delta y}\ ,\ \frac{\partial \mu}{\partial y}=\frac{\mu_{j+1}-\mu_{j-1}}{2\Delta y}$$

By substituting the "Eq. (16-17)" within the "Eq. (8)", the two-dimensional equation of wave propagation in a functionally graded plate is reduced to a finite difference equation in "Eq. (18 and 19)":

$$u_{i,j}^{k+1}=\frac{(\Delta t)^2}{\rho_{i,j}}\left\{\begin{array}{l}(\lambda_{i,j}+2\mu_{i,j})\left(\frac{u_{i+1,j}^{k}-2u_{i,j}^{k}+u_{i-1,j}^{k}}{(\Delta x)^2}\right)+\mu_{i,j}\left(\frac{u_{i,j+1}^{k}-2u_{i,j}^{k}+u_{i,j-1}^{k}}{(\Delta y)^2}\right)+\\ (\lambda_{i,j}+\mu_{i,j})\left(\frac{v_{i+1,j+1}^{k}-v_{i-1,j+1}^{k}+v_{i-1,j-1}^{k}-v_{i+1,j-1}^{k}}{4\Delta x\Delta y}\right)+\left(\frac{\lambda_{i+1}-\lambda_{i-1}}{2\Delta x}+2\frac{\mu_{i+1}-\mu_{i-1}}{2\Delta x}\right)\times\\ \left(\frac{u_{i+1}-u_{i-1}}{2\Delta x}\right)+\left(\frac{\mu_{j+1}-\mu_{j-1}}{2\Delta y}\right)\left(\frac{u_{j+1}-u_{j-1}}{2\Delta y}+\frac{v_{i+1}-v_{i-1}}{2\Delta x}\right)+\left(\frac{\lambda_{i+1}-\lambda_{i-1}}{2\Delta x}\right)\left(\frac{v_{j+1}-v_{j-1}}{2\Delta y}\right)\end{array}\right\} \quad (18)$$
$$+2u_{i,j}^{k}-u_{i,j}^{k-1}$$

$$v_{i,j}^{k+1}=\frac{(\Delta t)^2}{\rho_{i,j}}\left\{\begin{array}{l}(\lambda_{i,j}+2\mu_{i,j})\left(\frac{v_{i+1,j}^{k}-2v_{i,j}^{k}+v_{i-1,j}^{k}}{(\Delta y)^2}\right)+\mu_{i,j}\left(\frac{v_{i,j+1}^{k}-2v_{i,j}^{k}+v_{i,j-1}^{k}}{(\Delta x)^2}\right)\\ +(\lambda_{i,j}+\mu_{i,j})\left(\frac{u_{i+1,j+1}^{k}-u_{i-1,j+1}^{k}+u_{i-1,j-1}^{k}-u_{i+1,j-1}^{k}}{4\Delta x\Delta y}\right)+\left(\frac{\lambda_{i+1}-\lambda_{i-1}}{2\Delta y}+2\frac{\mu_{j+1}-\mu_{j-1}}{2\Delta y}\right)\times\\ \left(\frac{v_{j+1}-v_{j-1}}{2\Delta y}\right)++\left(\frac{\mu_{i+1}-\mu_{i-1}}{2\Delta x}\right)\left(\frac{v_{i+1}-v_{i-1}}{2\Delta x}+\frac{u_{j+1}-u_{j-1}}{2\Delta y}\right)+\left(\frac{\lambda_{j+1}-\lambda_{j-1}}{2\Delta y}\right)\left(\frac{u_{i+1}-u_{i-1}}{2\Delta x}\right)\end{array}\right\} \quad (19)$$
$$+2v_{i,j}^{k}-v_{i,j}^{k-1}$$

## 4 RESULTS AND DISCUSSION

To study the wave propagation in two dimensions in a plate made of FGM materials, a plane strain media with a square cross section is considered as follows. The Cartesian coordinates $x$ and $y$ along the longitudinal and transverse are shown in "Fig. 6" .

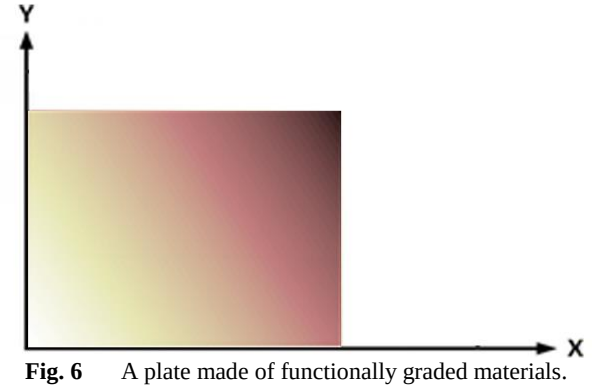


**Fig. 6** A plate made of functionally graded materials.

In "Fig. 7" , we select ABCD on the plate and examine it. In this figure, there are also points that are shown for getting data and comparing the selected results.

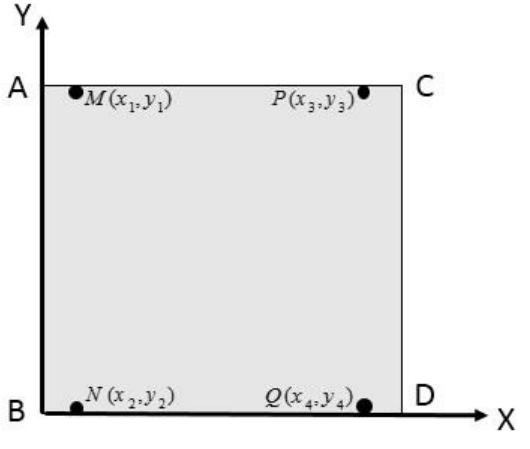


**Fig. 7** Selected points for getting data.

**First case**

As in the previous section noted, the first case of materials distribution is considered as a power law function. In this case, the dimensions of the plate are considered as square (1 m × 1 m).

The coordinates of the data points are assumed in this case as "Table 1" .

**Table 1** The coordinates of the selected points

| | P | M | N | Q |
|---|---|---|---|---|
| X(m) | 0.8 | 0.2 | 0.2 | 0.8 |
| Y(m) | 0.8 | 0.8 | 0.1 | 0.1 |

The properties of the two-dimensional FG plate are also defined in the "Table 2" .

**Table 2** Material properties of functionally graded plate

| Constituents | Material | E(GPa) | $\rho$ $(\frac{kg}{m^3})$ | $\nu$ |
|---|---|---|---|---|
| $m_1$ | Ti6Al4 V | 115 | 4515 | 0.31 |
| $m_2$ | Al1100 | 69 | 2715 | 0.33 |
| $c_1$ | Sic | 440 | 3210 | 0.14 |
| $c_2$ | $Al_2O_3$ | 150 | 3470 | 0.21 |

In this case, the volume fraction chart is depicted for the four materials in the FG plate for $n_x = n_y = 1$.

As shown in the diagrams in "Fig. 8" , the distribution of materials is linearly from zero to 1, and also according to "Fig. 7" , it is determined that point A of C2, point B of C1, point C of M2 and the point D of M1.

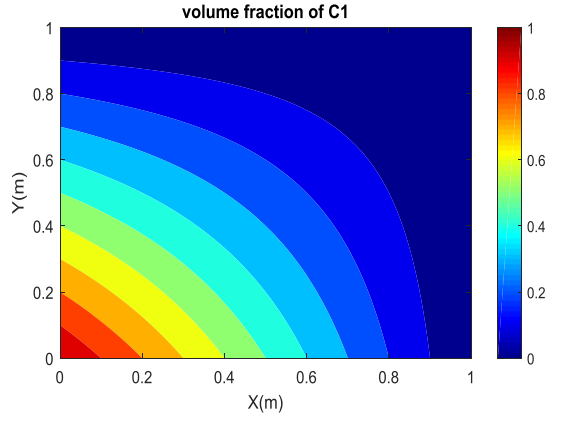


**(a)**

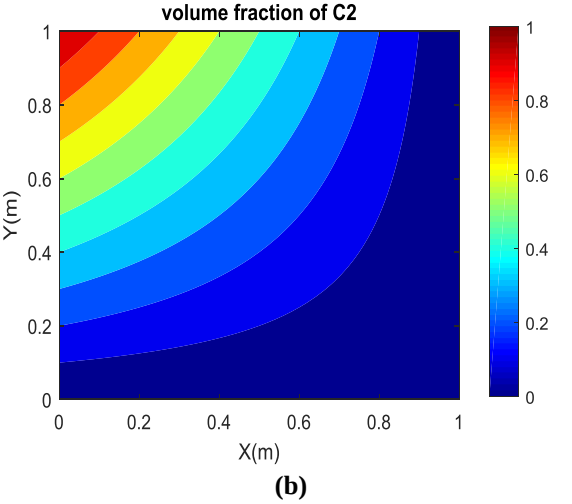


**(b)**

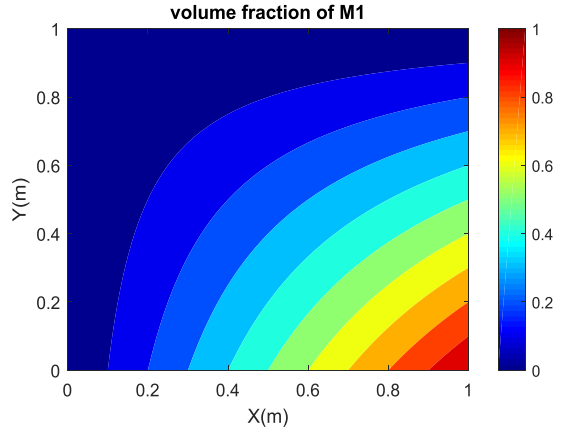


**(c)**

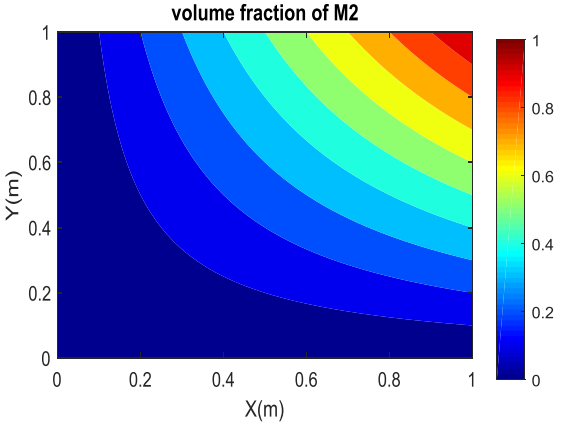


**(d)**

**Fig. 8** Variation of volume fraction of materials in first case.

In order to verify the results, the plate is assumed to be homogeneous. This assumption is obtained by inserting $n = 0$ in "Eq. (1)" and also the stress applied to the plate is considered as a two-dimensional wave. The specification of the material used for the homogeneous plate is given in "Table 3" .

**Table 3.** Mechanical properties of plate for homogeneous state

| Material | E(GPa) | $\rho(kg / m^3)$ | $\nu$ |
|---|---|---|---|
| Ti6Al4 V | 115 | 4515 | 0.31 |

In order to ensure the equations and results obtained, the displacement value at a point in the network is compared in "Fig. 9" with the results of the research using the two-dimensional wave theory that is calculated analytically by the method of separation of variables in [24] and [25].

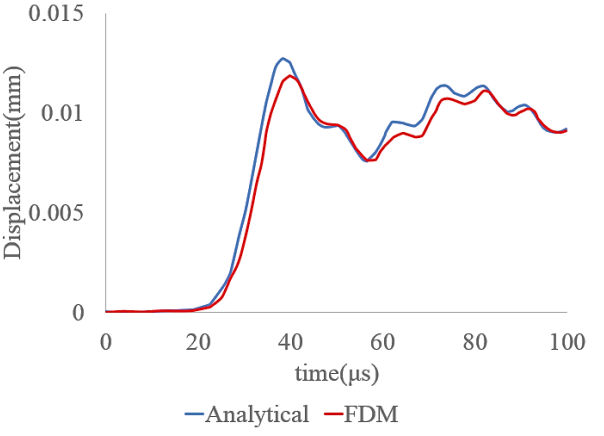


**Fig. 9** Validation Chart for a point in the network.

In "Fig. 10" , the graphs of the displacements in the direction $x$ and $y$ , namely $u, v$ displacements for the $n_x$ = 1, 0.2, 10 and $n_y$ = 1, 0.4, 10 are plotted.

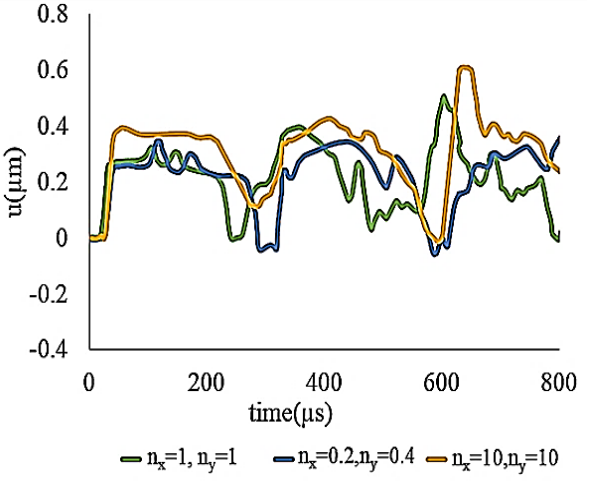


**(a)**

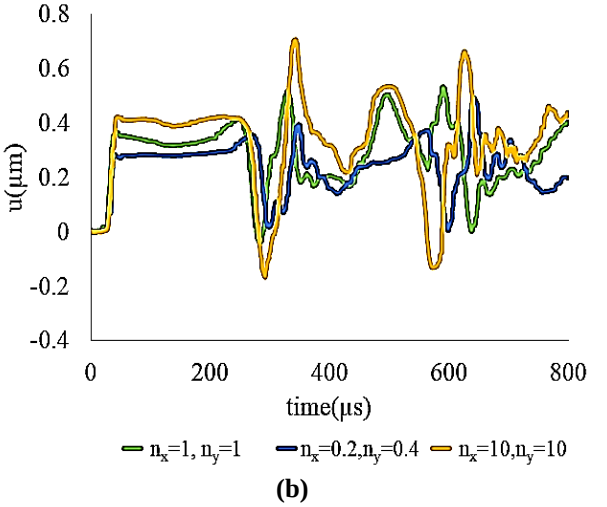


**(b)**

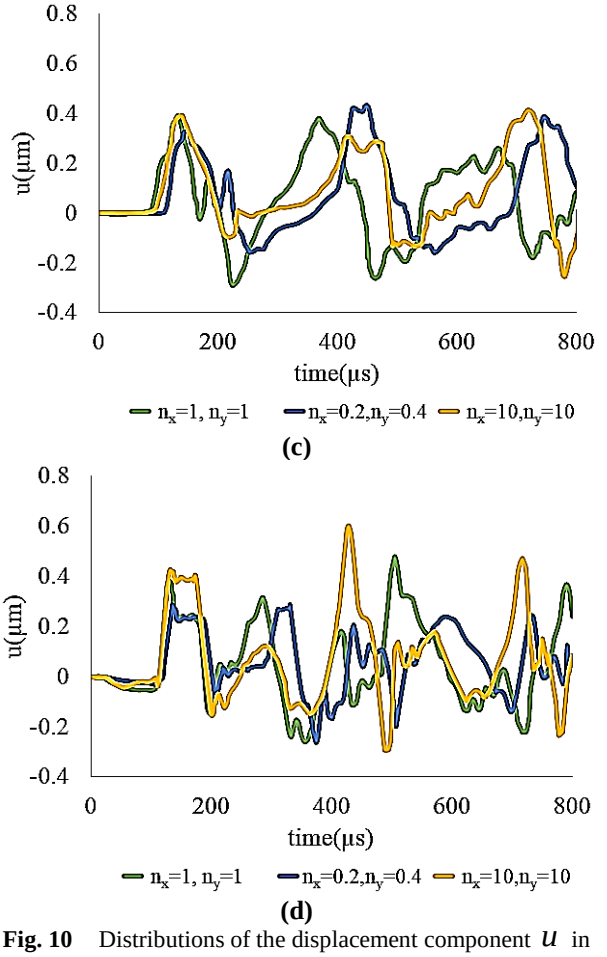


**Fig. 10** Distributions of the displacement component $u$ in terms of time for the points: (a): M, (b): N, (c): P, and (d): Q in first case.

According to "Fig. 10" , because of the point N located on the waves of two stresses at a time, it can be seen that the maximum displacement of u at the point N and the volume fraction 10 is 0.7 µm. As well as the role of the volume fractional power, in $n$ = 10, it is possible to place more ceramics than metal at this point. At point *Q*, the conditions are like the point N. Also in the volume fraction 10, the maximum displacement is as high as 0.6 µm and the minimum displacement is as high as 0.1 µm.

It is worth mentioning that $n_x$ = 0.2 and $n_y$ = 0.4 are considered for drawing graphs that in the interval of different volume fraction, using the minimum function of MATLAB software, the appropriate volume fraction to detect the effective optimal stress is searched. Finally, the two volume fractions indicated with the following stress are considered as the most appropriate option:

$$\sigma_{eff} = 2.4548 \times 10^{6} \text{ pa} = 2.4548 \text{ Mpa}$$

In the following, according to "Fig. 11" , displacement ($v$) variation in time charts are plotted for $n_x$ = 1, 1, 10, separated by points M, N, P, and Q.

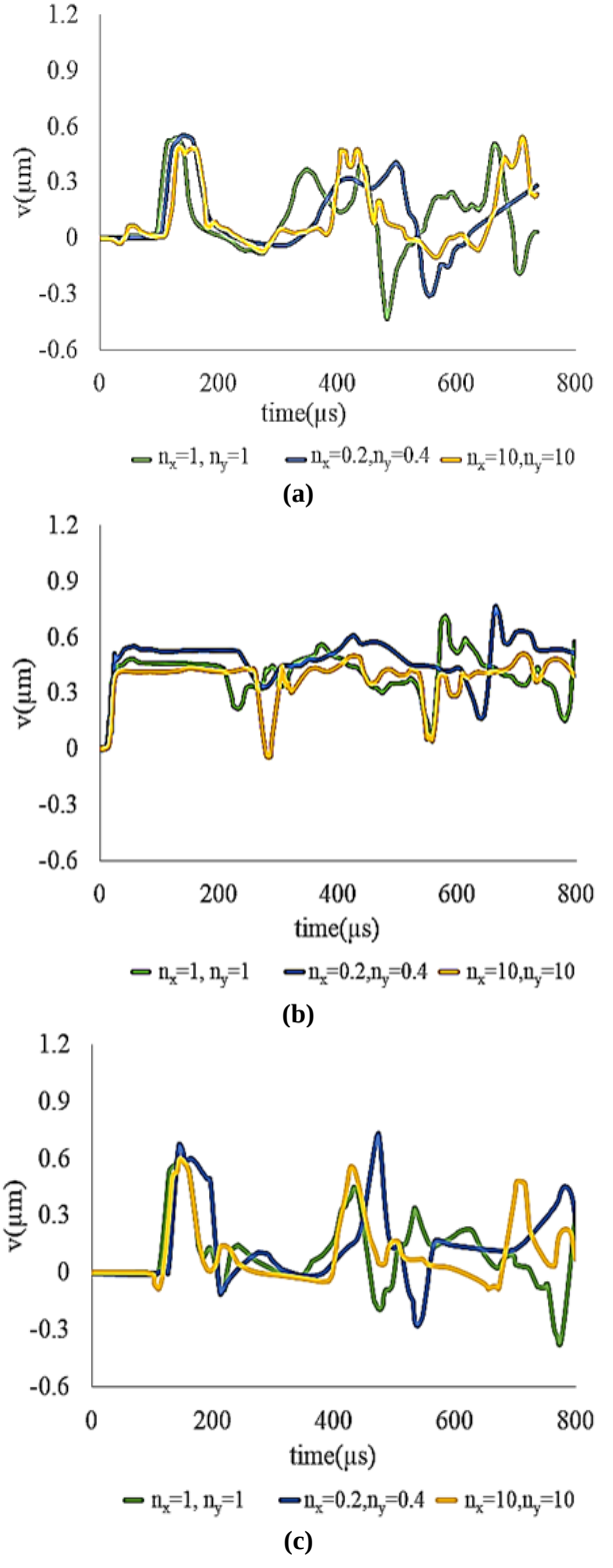

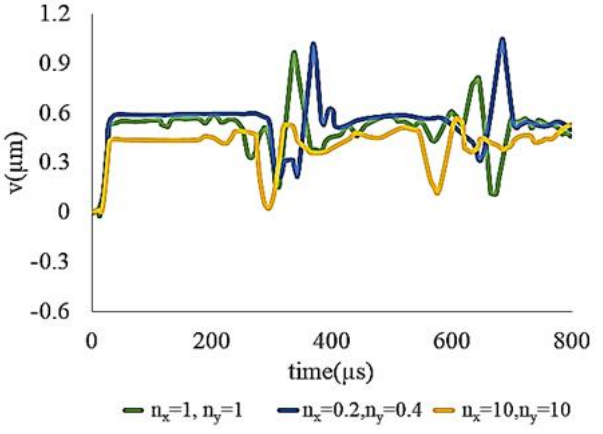


**(d)**

**Fig. 11** Distributions of the displacement component $v$ in terms of time for the points: (a): M, (b): N, (c): P, and (d): Q in first mode.

According to "Fig. 11", it can be seen that the maximum displacement along y direction is related to the point Q, occurred at $n_x$ = 0.2, $n_y$ = 0.4 and equal to approximately 1 μm. The reason for this is the position of the point Q in the path of the shock wave and also the volume fraction power in y direction in relation to x direction is higher. In "Fig. 12", the strain variation graphs in terms of time are plotted separately for the four-point M, N, P and Q.

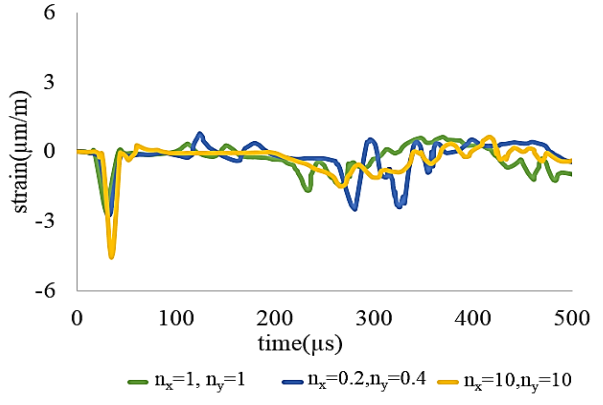


**(a)**

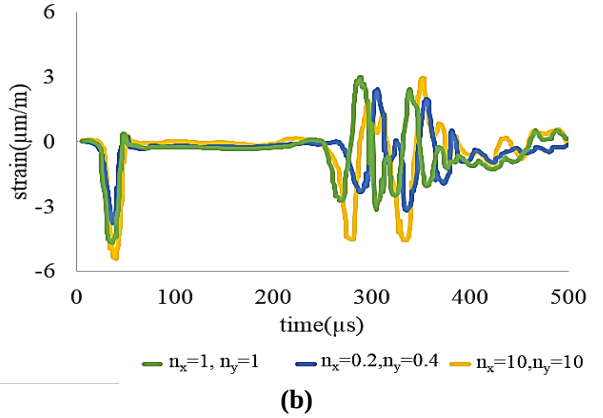


**(b)**

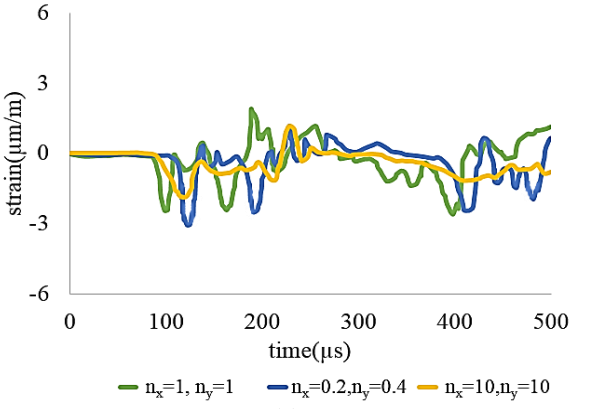


**(c)**

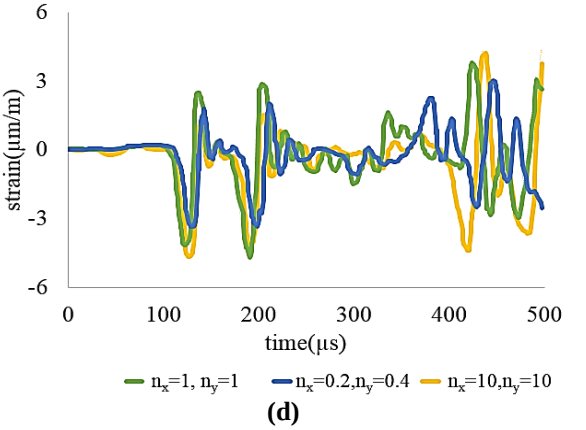


**(d)**

**Fig. 12** Distributions of the strain in terms of time for the points: (a): M, (b): N, (c): P, and (d): Q in first mode.

With respect to "Fig. 12", we can find that the maximum strain occurs at the points N and Q, in the volume fraction $n=10$. At the point N, the maximum strain was -5.3 μm/m. As we know, negative strain means compression. The reason for this is that this point is located at the beginning of the propagation path of two stress wave. Also, the volume fraction power also influences the exacerbation of this event, that way, in $n_x = n_y = 10$, the point N is of the sic type, and this causes an increase in the strain value at this point. In "Fig. 13", the stress charts are plotted for four points:

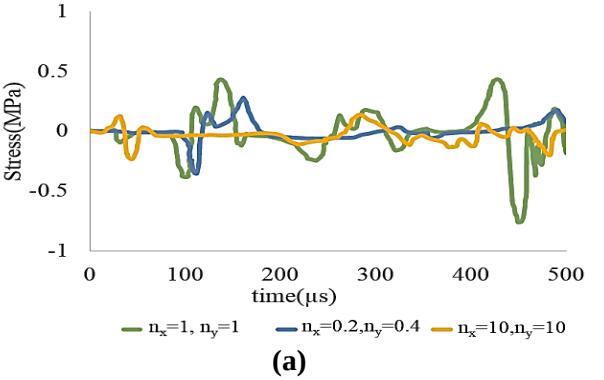


**(a)**

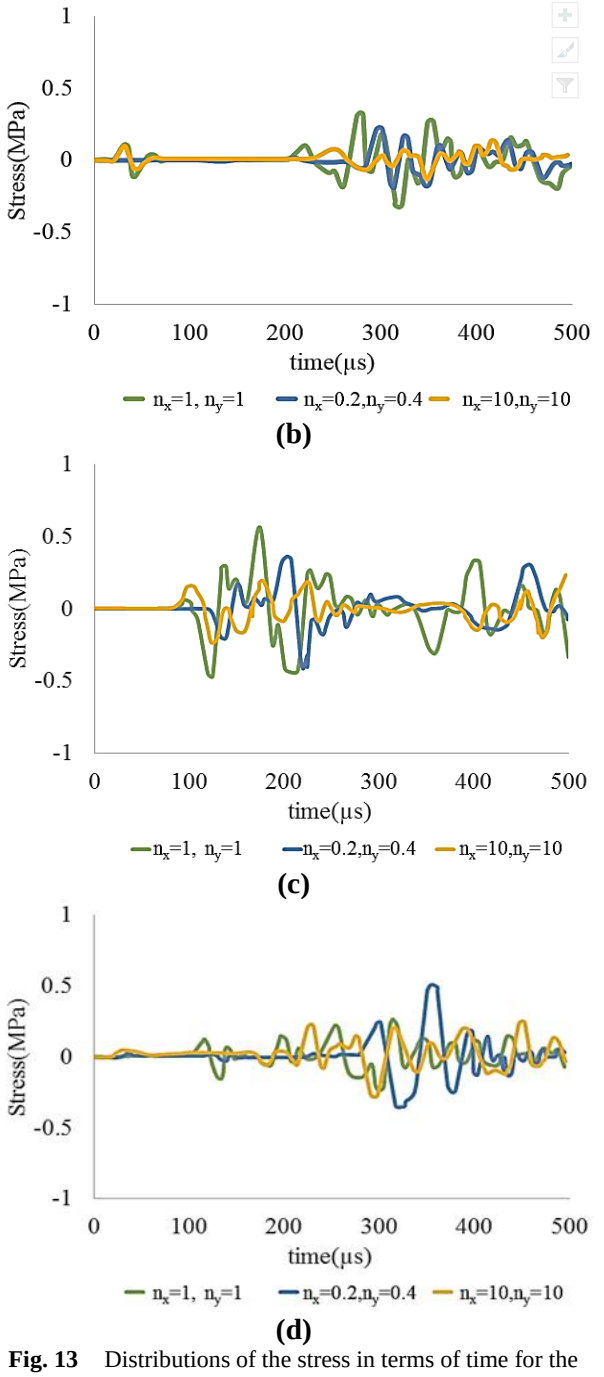


**Fig. 13** Distributions of the stress in terms of time for the points: (a): M, (b): N, (c): P and, (d): Q in first mode.

As shown in "Fig. 13" , the highest stress occurred in this case is related to the point M and the lowest stress is also related to the point N. Also, at points, M, N, P, the highest stress was in the state $n_x = n_y = 1$ and the lowest stress was in the state $n_x = 0.2$, $n_y = 0.4$, but at the point Q, the maximum stress value occurs in the state $n_x = 0.2$, $n_y = 0.4$ and the minimum stress value occurs in the state $n_x = n_y = 1$. The reason for this is that the linear distribution of the material in the plate causes a lot of stress in the body, but if we consider the volume fractional power in decimal form and the distribution of the material according to it, then we will have a better combination of materials in every place, and this will reduce the stress at any point in the plate. Of course, it should be noted that at point Q, due to the effects of a recurrence wave in the time interval of 300 to 400 μs, the volume fraction $n_x = 0.2$, $n_y = 0.4$ has recorded the highest stress.

In "Fig. 14" , the von Mises stress-time graphs are plotted separately for the four-point M, N, P and Q.

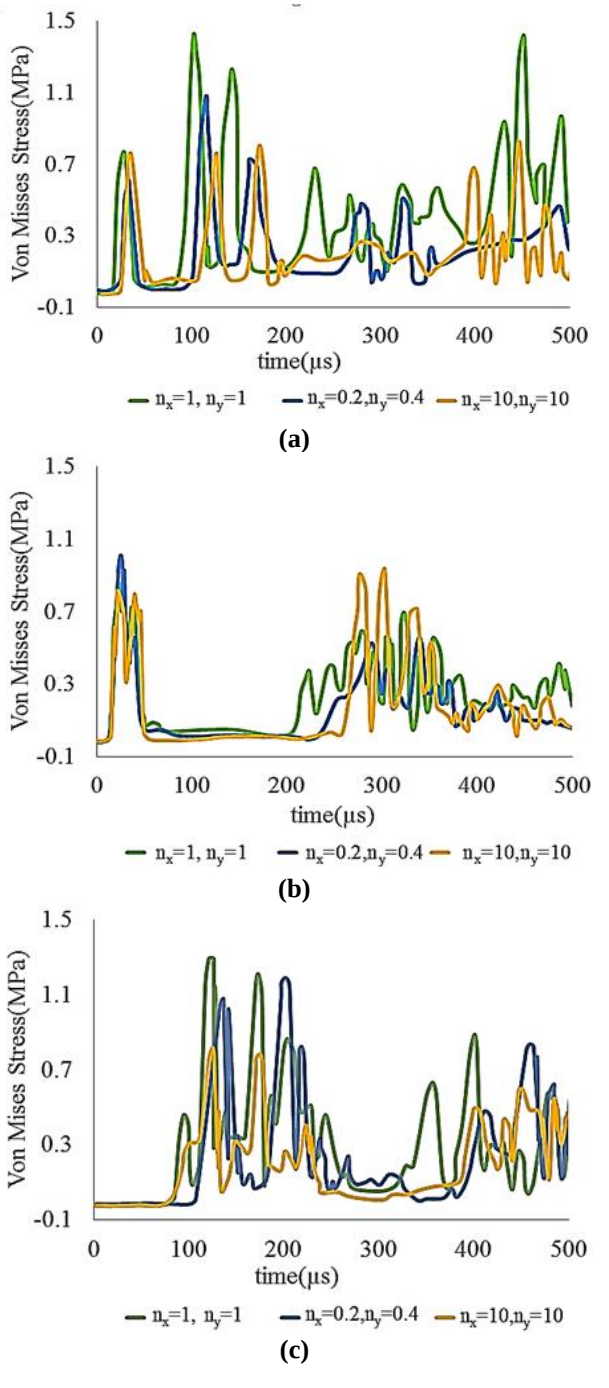

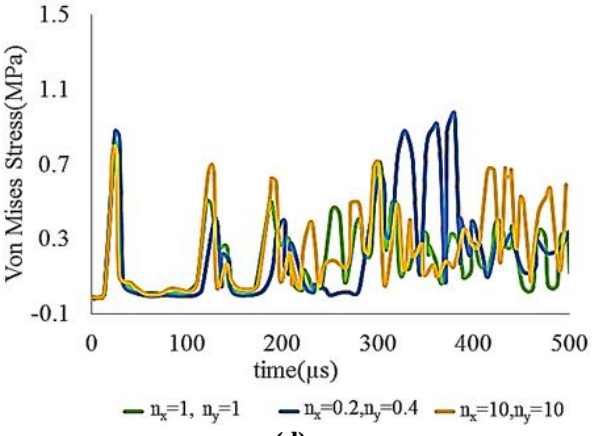


**(d)**

**Fig. 14** Distributions of the von Mises stress in terms of time for the points: (a): M, (b): N, (c): P and, (d): Q in first mode.

According to "Fig. 14" , the maximum von Mises stress value occurred at the point M in the state. Given that the point M is at the beginning of the path of wave motion, and also the distribution of the volume fraction that caused the lower amount of the first metal (m1) to be placed at this point, it was expected to witness the highest stress at this point. At the point *N*, as expected, in the $n_x$ = 0.2, $n_y$ = 0.4 except for the first moments, in the remaining moments, minimum value of von Mises stress was reported. At the point P, the lowest stress value was observed in $n_x = n_y = 10$, which is due to the distribution of the volume fraction of the material and the location of this point in the return wave path.

**Second case**

As stated in the previous section, another mode of distribution of the volume fraction of the material in the functionally graded plate is obtained with having the volume fraction in 4 points of the network and derivatives *xy*, *y*, *x* by using the "Eq. (3)" . A possible model of distribution of the volume fractions of 4 materials in the FG plate is shown in "Fig. 15" .

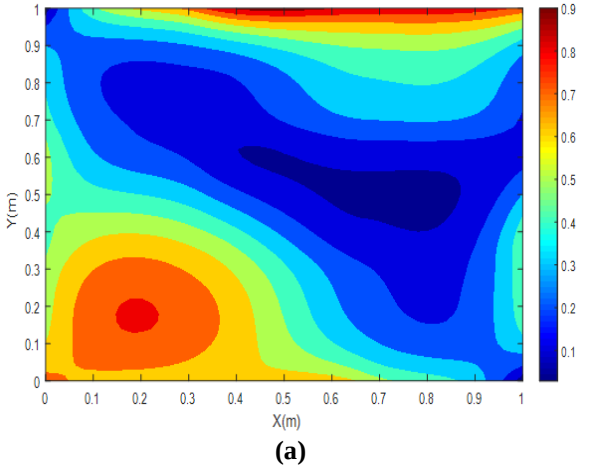


**(a)**

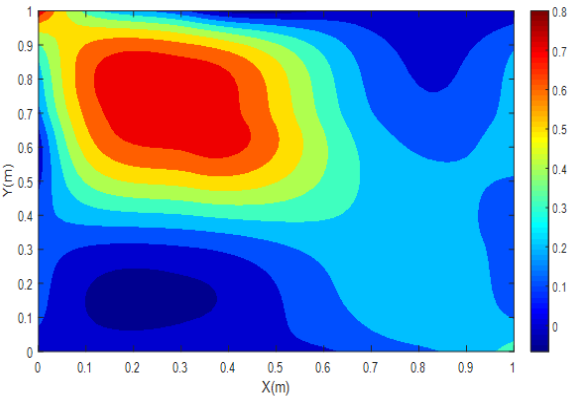


**(b)**

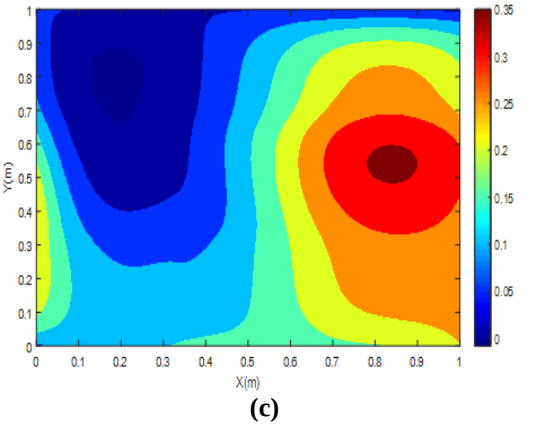


**(c)**

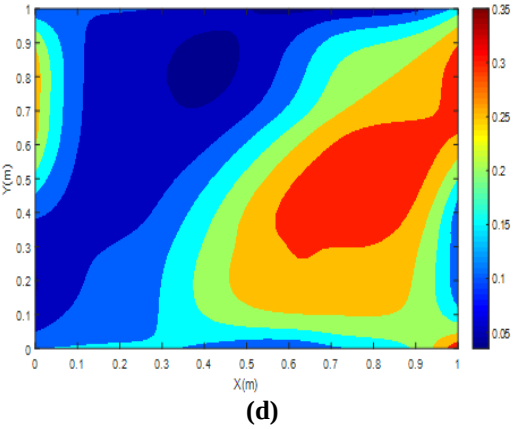


**(d)**

**Fig. 15** Variation of volume fraction for the four materials in second mode.

In the following, we use a single objective genetic algorithm to optimize the distribution of materials. This algorithm is used to optimize the placement of functionally graded material together in order to achieve a main stress or von Mises stress to the minimum value in functionally graded plate.

For this purpose, the objective function of the algorithm is defined as follows:

$$F(X) = F(V_i) = \sigma_{vonmises}(x, y, t)$$

It should be noted that the algorithm's constraints in the present study are defined in two states:
1- Input Constraints:

$$V_{m1}+V_{m2}+V_{c1}+V_{c2}=1$$

$$0\le V_{c2}\le 1, 0\le V_{c1}\le 1, 0\le V_{m1}\le 1, 0\le V_{m2}\le 1$$

2- Output Constraints:

$$\max\{\sigma_{vonmises}\}\le\sigma_y$$

Following the implementation of the single-objective genetic algorithm in MATLAB software, the following results were obtained.
In the description of "Fig. 16" , it should be noted that at each repetition of the algorithm, the best person in the population has the best value for fitness of the objective function with the black point, and the average fitness of the entire population is determined by the blue color. As it is clear from the diagram, from the repetition of 150, the graph has converged, and at the last one, the 200th, the mean of fitness and the best fit are found to be equal. In the following, the optimal volume fraction distribution for 4 materials is presented.

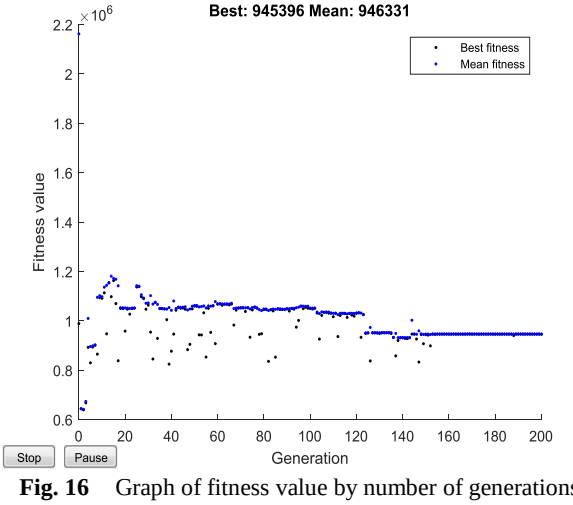


**Fig. 16** Graph of fitness value by number of generations (This plot has low quality).

According to "Fig. 17" , the optimal distribution of volume fractions obtained will cause the minimum value of concentration stress at any point in the network. The correctness of this claim is examined by plotting the von Mises stress diagram for an arbitrary point in the network compared to the volume fraction in the first mode.

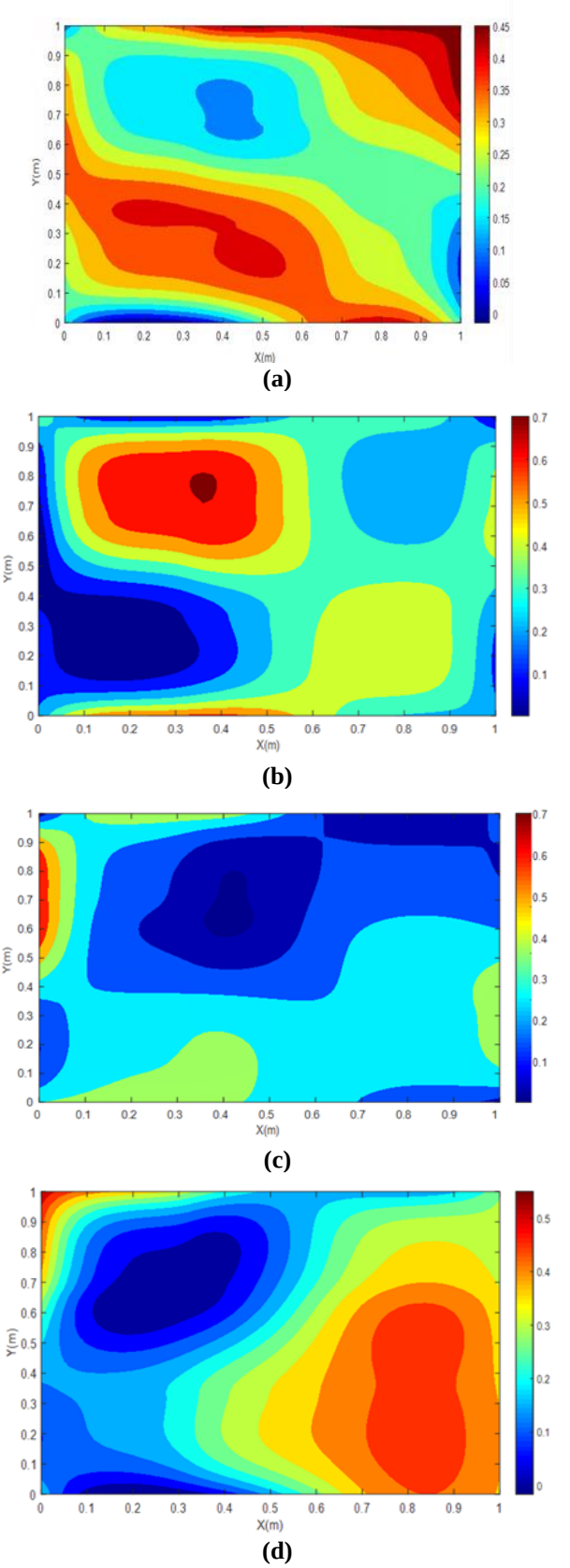


**(a)** **(b)** **(c)** **(d)**

**Fig. 17** Optimal distribution of the volume fraction of the functionally graded material.

As it is shown in "Fig. 18" , von Mises stress variations have experienced a significant loss in optimal mode than variations in various volume fractions. Therefore, it can be concluded that by designing a volume fraction of functionally graded materials optimally, access to a lower concentration of stress in these materials is provided.

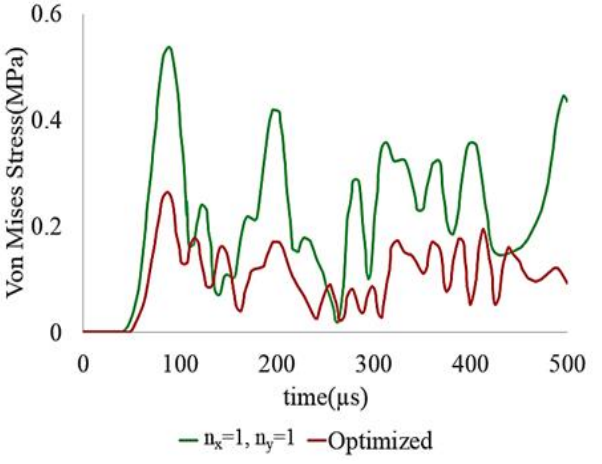


**(a)**

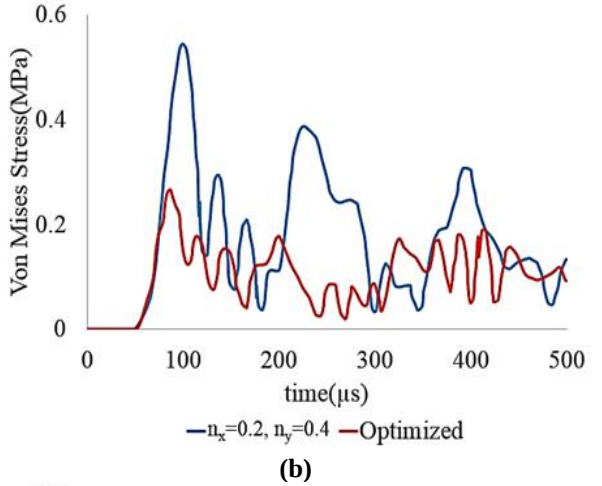


**(b)**

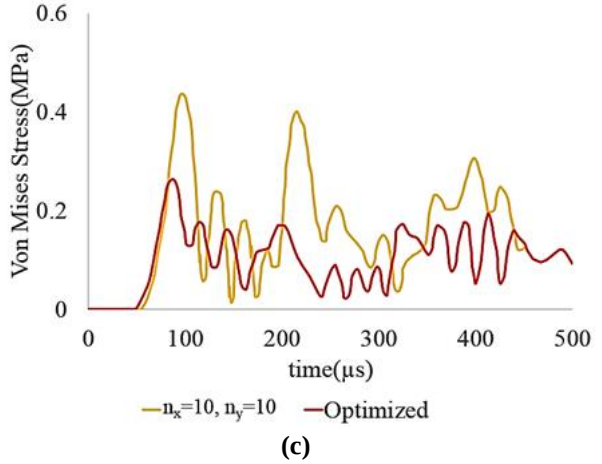


**(c)**

**Fig. 18** Comparison of von Mises stress in optimum with volume fraction power.

## 5 CONCLUSION

The main purpose of this study was to analyze and optimize the effect of materials distribution on a functionally graded plate. Generally, according to the obtained results, it is clear that any variation in the properties of the materials causes significant changes in the amount of stress produced by longitudinal waves. Also, variation of displacement and strain are no exception. According to the material properties changes in two directions, the variation of stress and strain are different in all points. So firstly, research was conducted on the propagation of a wave on a FG plate whose properties have been linearly changed, and stresses, strains and displacements have been studied. Then, with optimization, we see less stress reduced in different parts of the FG plate.

## REFERENCES

[1] Mahamood, R. M., Akinlabi, E. T., Shukla, M., and Pityana, S., Functionally Graded Material: an Overview, 2012.

[2] Huang C. Y., Chen, Y. L., Design and Impact Resistant Analysis of Functionally Graded Al2O3–ZrO2 Ceramic Composite, Materials & Design, Vol. 91, 2016, pp. 294-305.

[3] Daneshjou, K., Bakhtiari, M., and Tarkashvand, A., Wave Propagation and Transient Response of a Fluid-Filled FGM Cylinder with Rigid Core Using the Inverse Laplace Transform, European Journal of Mechanics-A/Solids, Vol. 61, 2017, pp. 420-432.

[4] Dorduncu, M., Apalak, M. K., and Reddy, J. N., Stress Wave Propagation in Adhesively Bonded Functionally Graded Cylinders: an Improved Model, Journal of Adhesion Science and Technology, Vol. 33, No. 2, 2019, pp. 156-186.

[5] Nikolarakis, A. M., Theotokoglou, E. E., Transient Analysis of a Functionally Graded Ceramic/Metal Layer considering Lord-Shulman Theory, Mathematical Problems in Engineering, 2018.

[6] Salehi Kolahi, M. R., Karamooz, M., and Rahmani, H., Elastic Analysis of Shrink-Fitted Thick FGM Cylinders Based on Linear Plane Elasticity Theory, Mechanics of Advanced Composite Structures, Vol. 7, No. 1, 2020, pp. 121-127.

[7] Goupee, A. J., Vel, S. S., Two-Dimensional Optimization of Material Composition of Functionally Graded Materials Using Meshless Analyses and a Genetic Algorithm, Computer Methods in Applied Mechanics and Engineering, Vol. 195, No. 44-47, 2006, pp. 5926-5948.

[8] Zhang, Z. J., Paulino, G. H., Wave Propagation and Dynamic Analysis of Smoothly Graded Heterogeneous Continua Using Graded Finite Elements, International Journal of Solids and Structures, Vol. 44, No. 11-12, 2007, pp. 3601-3626.

[9] Hosseini zad, S. K., Shakeri, M., Finite Difference Simulation of Elastic Wave Propagation in

Continuously Nonhomogeneous Materials, eighteen Annual International Conference on Mechanical Engineering-ISME, 2010.

[10] Cao, X., F. Jin, F., and Jeon, I., Calculation of Propagation Properties of Lamb Waves in A Functionally Graded Material (FGM) Plate By Power Series Technique, NDT & E International, Vol. 44, No. 1, 2011, pp. 84-92.

[11] D. Sun, D., Luo, S. N., Wave Propagation And Transient Response of a Functionally Graded Material Plate Under a Point Impact Load in Thermal Environments, Applied Mathematical Modelling, Vol. 36, No. 1, 2012, pp. 444-462.

[12] Noh, Y., Kang, Y., Youn, S., Cho, J., and Lim, O., Reliability-Based Design Optimization of Volume Fraction Distribution in Functionally Graded Composites, Computational Materials Science, Vol. 69, 2013, pp. 435-442.

[13] Zafarmand, H., Kadkhodayan, M., Three Dimensional Dynamic Analysis and Stress Wave Propagation in Thick Functionally Graded Plates Under Impact Loading, Modares Mechanical Engineering, Vol. 14, No. 11, 2015.

[14] Asgari, M., Material Optimization of Functionally Graded Heterogeneous Cylinder for Wave Propagation, Journal of Composite Materials, Vol. 50, No. 25, 2016, pp. 3525-3528.

[15] Bednarik, M., Cervenka, M., Groby, J., and Lotton, P., One-Dimensional Propagation of Longitudinal Elastic Waves Through Functionally Graded Materials, International Journal of Solids and Structures, Vol. 146, 2018, pp. 43-54.

[16] Amiri, A., Rahmani, H., and Balootaki, M. A., Torsional Wave Propagation in 1D and Two Dimensional Functionally Graded Rod, 2019. 10.22059/jcamech.2019.272234.350

[17] Yang, Y., Liu, Y., A New Boundary Element Method for Modeling Wave Propagation in Functionally Graded Materials, European Journal of Mechanics-A/Solids, Vol. 80, 2020, pp. 103897.

[18] Asemi, K., Salehi, M., and Akhlaghi, M., Three Dimensional Static Analysis of Two Dimensional Functionally Graded Plates, Int. J. Recent Adv. Mech. Eng.(IJMECH), Vol. 2, 2013, pp. 21-32.

[19] Vel, S. S., Pelletier, J. L., Multi-Objective Optimization of Functionally Graded Thick Shells for Thermal Loading, Composite structures, Vol. 81, No. 3, 2007, pp. 386-400.

[20] Yu, J., Lefebvre, J. E., and Zhang, C., Guided Wave in Multilayered Piezoelectric–Piezomagnetic Bars with Rectangular Cross-Sections, Composite Structures, Vol. 116, 2014, pp. 336-345.

[21] Auld, B. A., Acoustic Fields And Waves in Solids, Рипол Классик, 1973.

[22] Cherukuri, H., Shawki, T., A Finite- Difference Scheme for Elastic Wave Propagation in a Circular Disk, The Journal of the Acoustical Society of America, Vol. 100, No. 4, 1996, pp. 2139-2155.

[23] LeVeque, R. J., Finite Difference Methods for Ordinary and Partial Differential Equations: Steady-State and Time-Dependent Problems, Siam, 2007.

[24] Johnson, W., Impact Strength of Materials, 1983.

[25] Dawkins, P., Paul's OnLine Math Notes: Differential Equations, ed, 2016.